Iron-rich particles in heavily contaminated multicrystalline silicon wafers and their response to phosphorus gettering

2012 Semicond. Sci. Technol. 27 125016

(http://iopscience.iop.org/0268-1242/27/12/125016)

Semicond. Sci. Technol. **27** (2012) 125016 (5pp) doi:10.1088/0268-1242/27/12/125016

Iron-rich particles in heavily contaminated multicrystalline silicon wafers and their response to phosphorus gettering

D Macdonald[1], S P Phang[1], F E Rougieux[1], S Y Lim[1], D Paterson[2], D L Howard[2], M D de Jonge[2] and C G Ryan[3]

[1] Research School of Engineering, College of Engineering and Computer Science, The Australian National University, Canberra ACT 0200, Australia
[2] Australian Synchrotron, 800 Blackburn Rd, Clayton, Victoria 3168, Australia
[3] CSIRO Earth Science and Resource Engineering, Clayton, Victoria 3168, Australia

E-mail: daniel.macdonald@anu.edu.au

Received 23 August 2012
Published 5 November 2012
Online at stacks.iop.org/SST/27/125016

Abstract
Heavily contaminated multicrystalline silicon wafers have been studied using a scanning synchrotron x-ray fluorescence micro-probe, revealing the presence of iron-rich particles located along grain boundaries. These particles were found to be partially dissolved and removed during phosphorus gettering treatments at 900 or 1000 °C for times of up to 100 min, with increased gettering efficiency at higher temperatures and times. Annealing without the phosphorus gettering layer present at the wafer surfaces resulted in no discernible reduction in particle coverage, showing that the gettering layer is essential in such heavily contaminated wafers, in order to reduce the dissolved Fe concentration below the solubility limit, and therefore allow dissolution to proceed.

1. Introduction

Metallic impurities are omnipresent in multicrystalline silicon for solar cells, due primarily to contamination from the crucibles that contain the ingots during crystallization [1, 2]. The distribution and chemical nature of these metallic impurities are critically important in determining the performance of solar cells made with such material. Iron silicide is perhaps the most common and important metallic precipitate found in multicrystalline silicon [3]. In wafers from the central parts of mc-Si ingots, it is usually present as particles tens of nanometres in size that form at grain boundaries during ingot cooling [3, 4]. Previous work has shown that these particles can dissolve during processing, releasing interstitial iron into the wafer bulk, and thus degrading the bulk carrier lifetime [5, 6]. They also act as strong recombination sites in their own right [7]. These studies have used high resolution nano-probe synchrotron x-ray fluorescence (SXRF), which is sufficiently sensitive to detect such small particles. However, the small beam size required (typically of the order of 100 nm) means that only relatively small regions of samples can be studied. This often means that repeated measurements on the same particles are needed to draw meaningful conclusions about the impact of cell processing steps such as thermal annealing.

In this work, we apply a rapid scanning SXRF micro-probe to map the presence of metallic particles in mc-Si wafers over large areas in relatively short periods of time. This allows measurement of many tens or hundreds of particles in each sample, thereby enabling meaningful comparisons between neighbouring samples cut from the same wafer that have undergone different processing steps. However, the use of a micro-probe rather than a nano-probe reduces the measurement sensitivity when probing particles smaller than the spot size, due to the smaller fraction of the probed volume occupied by the particles. The faster scan speed further reduces sensitivity. Consequently, the use of a micro-probe is more effective in heavily-contaminated wafers, which usually also

contain larger particles, noting however that sensitivity to smaller particles can be regained through the use of a high efficiency detector system. Therefore, we have applied the micro-probe to wafers from very close to the very bottom of a mc-Si ingot, which contain iron precipitates that are easily detectible with this technique. Using this approach, we demonstrate that phosphorus gettering at temperatures of 900 °C and above can significantly reduce the number of precipitates present in this material, even though they are larger than the particles typically found in central mc-Si wafers.

2. Experimental methods

The wafer studied in this work was from a standard industrially-grown, directionally-solidified boron-doped p-type multicrystalline silicon ingot made with electronic-grade silicon feedstock. After solidification, some material was trimmed off the top, bottom and edges of the ingot prior to wafering, in order to avoid possible damage to the wire saw caused by hard inclusions in the very edge regions. Nevertheless, the remaining material still exhibits very low-lifetime regions at the edges of the ingot, and in wafers from the bottom and top of the ingot. These low-lifetime regions have been well documented in the literature [2, 8]. The wafer studied here was from the very bottom of the trimmed ingot, and approximately 1 cm from the bottom of the untrimmed ingot, and so within the contaminated region, with a bulk carrier lifetime well below 1 μs. The wafer exhibited small grains, in the range of 1 mm, as opposed to grains of several cm within the central regions of the ingot.

The 100 mm × 100 mm, 300 μm thick, square wafer was cut into 10 mm × 10 mm pieces which were chemically etched and cleaned to remove saw damage and surface contamination. The wafers were then annealed in a phosphorus-rich atmosphere ($POCl_3$ with O_2 and N_2), leading to a phosphorus diffusion on both surfaces of varying sheet resistance (depending on the time and temperature), at temperatures between 800 and 1000 °C, and for times between 10 and 100 min. The diffused layers were subsequently etched off prior to measurement with SXRF. Such phosphorus-diffused layers are known to efficiently getter dissolved Fe in Si [9].

The presence of the phosphorus gettering layer is potentially critical for such heavily contaminated material. The total concentration of Fe in a neighbouring wafer to that studied here has been measured previously by neutron activation analysis (NAA), and was found to be approximately 5×10^{14} cm^{-3} [10]. This value exceeds the solubility limit of Fe in silicon for the gettering temperatures used, which is equal to 3×10^{12}, 4×10^{13} and 4×10^{14} cm^{-3} for temperatures of 800, 900 and 1000 °C, respectively [11]. Therefore, in the absence of an external gettering layer, in principle no dissolution of precipitates could occur. However, the presence of the phosphorus layer removes dissolved Fe from the wafer bulk during the high temperature step, reducing it well below the solubility limit, and thus, in principle allowing the dissolution of precipitates. The gettering process may then be limited either by the release (dissolution), diffusion, or capture of Fe at the gettering sites.

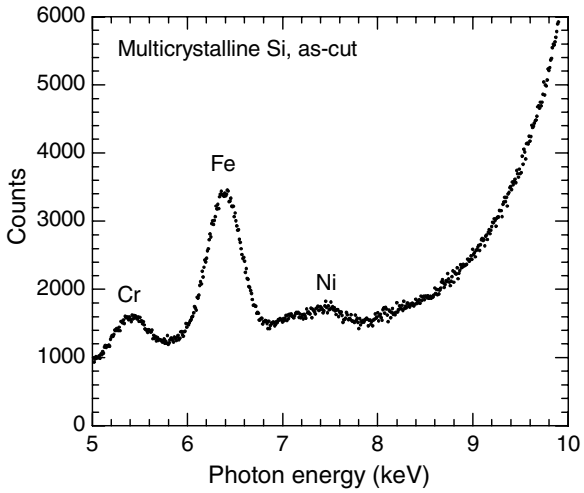

Figure 1. X-ray fluorescence spectrum from a region of a multicrystalline silicon wafer containing an Fe-rich particle, with traces of Cr and Ni. The large peak evident at 10 keV is caused by inelastic scattering of the incident beam.

The samples were analysed using the x-ray fluorescence microscopy (XFM) beamline at the Australian Synchrotron [12]. A photon energy of 12.7 keV was chosen, with a beam size of 2 μm and an intensity of approximately 10^{10} photons/s/μm^2 produced by a Kirkpatrick–Baez mirror microprobe. The sample was scanned at a constant speed of 0.5 mm s^{-1}, which yielded a scan rate of 16 min mm^{-2}, with a pixel size of 2 μm. The x-ray fluorescence was detected 'on-the-fly' with the Maia detector, a 384 element detector array and integrated spectroscopic imaging system [13, 14]. This arrangement has previously been shown to be well-suited to detecting metal particles in relatively heavily contaminated silicon feedstock materials for photovoltaics [15]. Here we apply it for the first time to mc-Si wafers. Data were subsequently processed using spectral de-convolution, background subtraction and projection of separated elemental images [16, 17]. De-convolution of the SXRF data used the dynamic analysis method [18, 19] and the GeoPIXE software suite [17].

The metallic impurities most commonly detected were Fe (Kα emission at 6.4 keV), Cr (5.4 keV) and Ni (7.5 keV). Figure 1 shows a typical SXRF spectrum from a region containing an Fe-rich particle, with traces of Cr and Ni present. However, for the majority of particles observed in this work, only Fe was detected, as demonstrated in figure 2, which shows a line-scan of the SXRF counts for these three elements across a pair of typical Fe-rich particles. Note that self-absorption by the Si lattice leads to an attenuation length of 36 μm for Fe Kα emission [20]. This limits the analysed volume within which Fe particles can be detected.

We performed scans of at least 6 mm^2 on each sample, resulting in a large number of Fe particles detected, typically between 40–200 particles. This is required to allow a meaningful comparison between neighbouring samples that had undergone different annealing conditions, without the

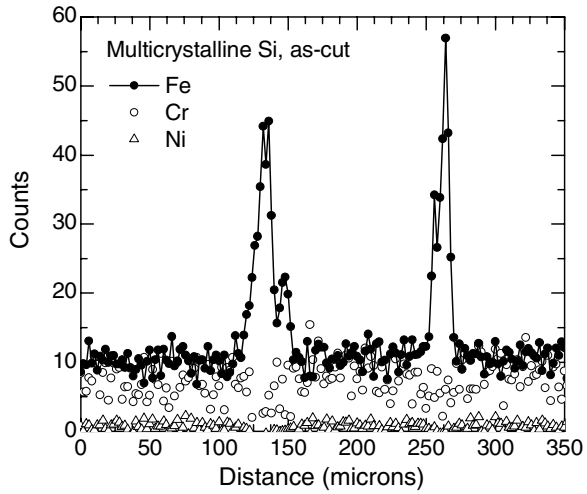

Figure 2. Line-scan of the SXRF peak intensities for Fe, Cr and Ni across two Fe-rich particles in an unprocessed multicrystalline silicon wafer.

need to re-measure the same sample before and after thermal processing, as discussed in more detail in the following section. Note that a scanned area of 6 mm^2 covers approximately ten complete grains and the associated grain boundaries. Conveniently, in this part of the ingot, the grains are quite uniform in size and shape, and evenly distributed across the wafer, much more so than in wafers from the central parts of an ingot, which have many large grains and some regions of small, highly dislocated grains.

There are a number of possible approaches to quantifying the distribution of Fe-rich particles in such samples based on SXRF maps. Recently, Fenning *et al* [21] used the estimated precipitate radius, in turn calculated from the number of Fe atoms detected in each particle, which, in combination with measurement on a suitable standard sample, is essentially proportional to the XRF counts per particle. Here we have used the simple metric of the proportion of the surface area covered by detected particles, determined using suitable image analysis software. Both of these approaches are preferable to using the number of particles, or particle density, since they give greater weight to larger particles, which contain more Fe.

In performing the particle analysis we defined a threshold count value in order to clearly distinguish particles from the background counts which were registered uniformly across the samples. Despite the much lower magnitude of these background counts per pixel, they nevertheless accounted for more than 99% of the total counts in our samples, due to the very small area coverage of the Fe particles. We observed that this background Fe level was very similar in all of our samples, and did not significantly change after phosphorus gettering, despite the removal of many of the particles by some of the gettering steps. This indicates that the background counts represent the sensitivity limit of the SXRF scans. Note that it is also possible, in principle, that the background counts reflect a uniform dissolved Fe concentration in our samples. However, the solid solubility limit of Fe in Si at the processing temperatures used here is expected to limit this concentration to values below 5×10^{14} cm^{-3}, which is well below the expected bulk detection limit of the SXRF arrangement.

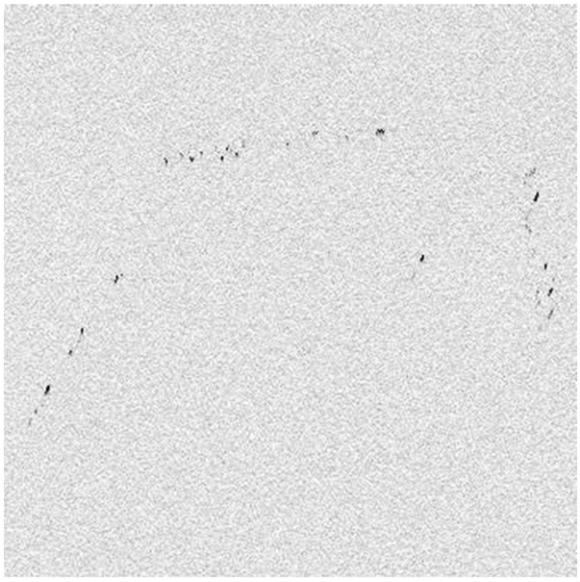

Figure 3. The map of Fe particles derived from SXRF spectra in a 0.72 × 0.72 mm region of an unprocessed multicrystalline silicon wafer. The majority of particles are aligned along grain boundaries, as indicated by the linear distributions.

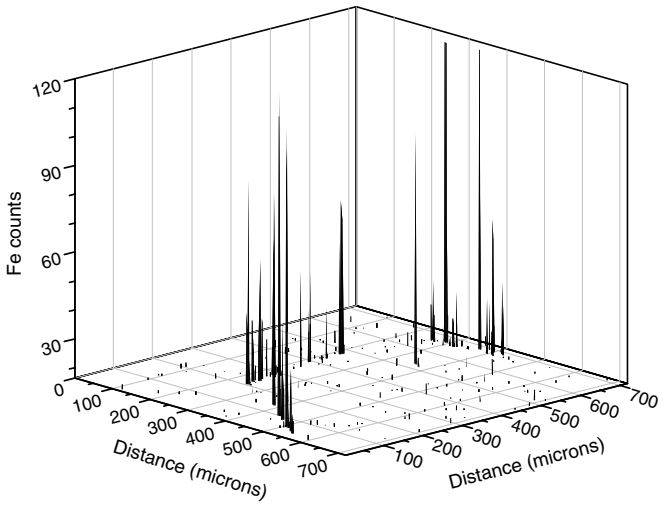

Figure 4. Surface plot of Fe SXRF emission intensity for the same region as shown in figure 3. The variations in peak intensity can be caused by different particle sizes and/or depths below the surface.

3. Results and discussion

Figure 3 shows a small section of a map of the Fe distribution in a sample that had received no thermal processing. The region shown is 0.72 mm × 0.72 mm in size, and is part of a larger 4 mm × 1.5 mm map. The larger 6 mm^2 map was found to contain 185 Fe particles, which covered 0.036% of the total mapped surface area. The image shows that the Fe rich particles are largely aligned along the grain boundaries, which was observed in all of the samples. Figure 4 shows a surface plot of the region in figure 3. This plot indicates that the particles vary not only in lateral size, but also in the intensity of the peak SXRF signal. This intensity variation can be caused both by differences in the particle sizes, or by differing depths

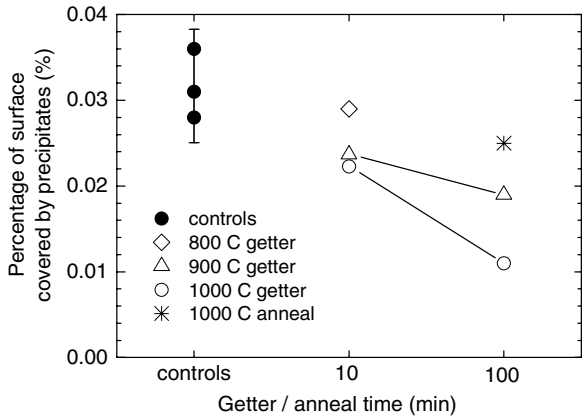

Figure 5. Percentage of the surface area covered by detected Fe-rich particles, for unprocessed control samples, and samples that were phosphorus gettered for 10 or 100 min at temperatures of 800, 900 and 1000 °C. The error bars for the control samples represent two standard deviations about the mean. Also shown is a sample annealed without gettering at 1000 °C for 100 min. The lines are guides to the eye.

of the particles, since the emission from particles further below the surface will be attenuated by absorption in the Si lattice, making them appear both smaller and less intense. In any case, if the depth distribution of the particles is random, as expected, the effect of differing particle depths will be averaged out over a sufficiently large number of sampled particles.

In order to assess the statistical reliability of comparing data from different samples which have undergone different treatments, we performed 6 mm^2 scans on three separate control samples which had received no thermal processing, and so in principle should have the same properties when measured over a large enough area. The results are shown in figure 5, which shows a plot of the percentage of the total surface area occupied by detected particles, both before and after phosphorus gettering at different temperatures, for a range of gettering times. For the three control samples shown on the left, the percentage of the surface covered by Fe particles was found to be 0.028%, 0.031% and 0.036%, with a standard deviation of 0.0033% absolute. The figure shows error bars that represent two standard deviations about the mean, approximating the 95% confidence interval. Subsequent data that falls outside this range can be considered likely to be statistically different to the control results. However, this estimate of the uncertainty in the data is itself uncertain, and we cannot rule out some additional impact of random variation from sample to sample on our results.

The results of the gettering experiments are summarized in figure 5. After gettering at 800 °C for 10 min, there was no significant reduction in the fraction covered by particles. However, for 900 and 1000 °C gettering, a downward trend is evident in the particle coverage as a function of gettering time, consistent with thermally activated dissolution of the particles. After 100 min gettering at 1000 °C, the Fe particles occupy only 0.01% of the sample surface. As expected, the number of particles was also reduced, dropping from around 30 particles mm^{-2} in the samples with no gettering treatment, to 12 particles mm^{-2} in the 1000 °C, 100 min gettered sample. These results show that even after such a long and high temperature gettering treatment, a significant proportion of the original particles remain, presumably due to the fact that they were sufficiently large at the beginning of the gettering process to remain undissolved.

In general, gettering processes may be limited either by the rate of impurity release (dissolution in this case), diffusion, or capture at the gettering sites. The diffusion energy of dissolved Fe in silicon allows much more rapid gettering of Fe than has been observed here, revealing that the process is not diffusion limited [9]. In addition, a capture limited process would normally exhibit a higher gettering effectiveness at 900 °C than at 1000 °C for phosphorus gettering of Fe in silicon, due to the temperature dependence of the solubility ratio between the wafer bulk and the diffused regions [9]. However, figure 5 shows that the higher temperature gives better gettering effectiveness in the samples studied here. Therefore we conclude that the gettering process is dissolution limited. Note that previous work by Zhang *et al* [22] on dissolution of Fe particles formed at oxygen precipitates in Czochralski-grown silicon wafers found effective dissolution within 10 min at 800 °C. It is clear therefore that the dissolution energy of the Fe particles located at the grain boundaries in multicrystalline wafers is much higher than for Fe particles located at oxygen precipitates.

Figure 5 also shows the result for a sample that was annealed in N_2 at 1000 °C for 100 min, but with no phosphorus gettering layer present. In this case, the Fe particles occupy 0.025% of the surface area, which is within two standard deviations of the non-annealed control samples. This confirms that the presence of the gettering layer is essential to reduce the dissolved Fe concentration in the wafer bulk below the solubility limit, therefore allowing the dissolution of the precipitates to proceed.

Both iron silicide and iron silicate particles have been observed before in mc-Si [1, 3]. However, iron silicide particles are mostly observed at grain boundaries, and are thought to form during ingot cooling, whereas as iron silicate particles are not likely to form during ingot growth, and probably originate from foreign inclusions in the melt. We therefore expect that the particles observed in this work are iron silicide, since they are aligned with the grain boundaries. As discussed above, iron silicide particles have been previously observed to dissolve during high temperature wafer processing. Note however that the particles in this work are significantly larger than those observed previously using nano-probes (<100 nm radius), and so are expected to take longer to dissolve, as we have indeed observed.

4. Conclusions

Synchrotron x-ray fluorescence (SXRF) maps of heavily contaminated multicrystalline silicon wafers reveal Fe particles located predominantly along the grain boundaries. These particles can be dissolved by high temperature phosphorus gettering, although some still remain even after gettering at 1000 °C for 100 min. Higher temperatures and longer gettering times result in a greater degree of dissolution

of the particles. Our results show that the presence of the phosphorus gettering layer during annealing is essential to allow particle dissolution to occur in such wafers, otherwise the wafer bulk remains saturated with dissolved Fe, impeding dissolution.

Acknowledgments

This research was undertaken on the x-ray Fluorescence Microscopy (XFM) beam-line at the Australian Synchrotron, Victoria, Australia. DM is supported by an Australian Research Council Future Fellowship FT110100680.

References

[1] Buonassisi T *et al* 2006 *Prog. Photovolt. Res. Appl.* **14** 513–31
[2] Olsen E and Øvrelid E J 2007 *Prog. Photovolt. Res. Appl.* **16** 93–100
[3] Buonassisi T *et al* 2005 *J. Appl. Phys.* **97** 074901
[4] McHugo S A *et al* 2001 *J. Appl. Phys.* **89** 4282–8
[5] Buonassisi T *et al* 2005 *Appl. Phys. Lett.* **87** 121918
[6] McHugo S A 1997 *Appl. Phys. Lett.* **71** 1984–6
[7] McHugo S A, Thompson A C, Perichaud I and Martinuzzi S 1998 *Appl. Phys. Lett.* **72** 3482–4
[8] Rinio M, Ballif C, Buonassisi T and Borchert D 2004 *Proc. of the 19th European Photovoltaic Solar Energy Conf. (Paris)* (Munich: WIP) pp 762–5
[9] Phang S P and Macdonald D 2011 *J. Appl. Phys.* **109** 073521
[10] Macdonald D, Cuevas A, Kinomura A, Nakano Y and Geerligs L J 2005 *J. Appl. Phys.* **97** 033523
[11] Istratov A A, Hieslmair H and Weber E R 1999 *Appl. Phys.* A **69** 13–44
[12] Paterson D *et al* 2011 *10th Int. Conf. on X-ray Microscopy; AIP Conf. Proc.* **1365** 219–22
[13] Ryan C G, Siddons D P, Moorhead G, Kirkham R, Dunn P A, Dragone A and Geronimo G D 2007 *Nucl. Instrum. Methods Phys. Res.* B **260** 1–7
[14] Ryan C G *et al* 2009 *J. Phys.: Conf. Ser.* **186** 012013
[15] Macdonald D, Rougieux F, Mansoulie Y, Tan J, Paterson D, Howard D L, de Jonge M D and Ryan C G 2010 *Phys. Status Solidi* a **207** 1807–10
[16] Ryan C G, Cousens D R, Sie S H, Griffin W L, Suter G F and Clayton E 1990 *Nucl. Instrum. Methods Phys. Res.* B **47** 55–72
[17] Ryan C G, Etschmann B E, Vogt S, Maser J, Harland C L, Achterbergh E v and Legnini D 2005 *Nucl. Instrum. Methods Phys. Res.* B **231** 183–8
[18] Ryan C G 2000 *Int. J. Imaging Syst. Technol.* **11** 219–30
[19] Ryan C G *et al* 2009 X-ray optics and microanalysis *Proc. 20th Int. Congress (Karlsruhe, Germany)* (New York: AIP) pp 9–17
[20] www.cxro.lbl.gov
[21] Fenning D P, Hofstetter J, Bertoni M I, Hudelson S, Rinio M, Lelièvre J F, Lai B, Cañizo C d and Buonassisi T 2011 *Appl. Phys. Lett.* **98** 162103
[22] Zhang P, Väinölä H, Istratov A A and Weber E R 2003 *Appl. Phys. Lett.* **83** 4324–6